University of Baghdad
College of Engineering
JE
JOURNAL OF ENGINEERING

Journal of Engineering

journal homepage: www.jcoeng.edu.iq

Volume 30 Number 8 August 2024

A PWM Adaptive Sliding Mode Observer for Charge Control of Lithium Ion Battery

Adeola Balogun[1], Chukwuemeka Sunday[1], Sunday Adetona[1,*], Sodiq Agoro[2], Frank Okafor[3]

[1]Department of Electrical and Electronics Engineering, University of Lagos, Lagos, Nigeria
[2]ABB Inc. Raleigh NC USA, NC, USA
[3]Nigerian Electricity Regulatory Commission, Abuja, Nigeria

ABSTRACT

An adaptive sliding mode control (SMC) based on PWM and an observer scheme for predicting the state of charge (SOC) of lithium-ion batteries is proposed. The control scheme is developed for a dc-dc buck converter used in regulated charge control of lithium-ion batteries. Unlike many estimation schemes where the converter's output voltage is predetermined and the nonlinearities ignored, the proposed scheme estimates the buck converter's output voltage, SOC, and nonlinearities in terms of errors in parameters. The stability of the proposed scheme is guaranteed by the Lyapunov method. The simulation was carried out in the Simulink in the MATLAB environment to transition from constant current charging mode to constant voltage charging mode. The results obtained from both modes in the Simulink in the MATLAB environment have shown that the dynamic control system of the SMC is asymptotically stable with excellent robust recovery features to sudden variations in input and un-modelled load.

Keywords: Adaptive sliding mode control, dc-dc converter, Lithium-ion battery, Lyapunov stability, State of charge.

1- INTRODUCTION

The proliferation of Lithium batteries in power applications in portable household and office devices, electric vehicles, space exploration, electric grid support etc., is due to the encouraging advantages lithium ion batteries have over other batteries (**Kim, 2010**); such as, relatively lighter weight, longer lifetimes, lower self-discharge rate, wider temperature operation range, smaller physical size, rapid charge capability, lower steady-state flow current, higher power density when compared to lead acid. However, the reliability and cost efficiency of the battery in different applications are directly influenced by the control

*Corresponding author
Peer review under the responsibility of University of Baghdad.
https://doi.org/10.31026/j.eng.2024.08.01

Article received: 28/05/2024
Article revised: 24/07/2024
Article accepted: 29/07/2024
Article published: 01/08/2024

schemes deployed to achieve energy and battery management strategies. In order for such schemes to make optimal decisions an accurate prediction of the battery state of charge (SOC) is required; and this is defined as the stored charge that is available for work relative to that which is available after the battery has been fully charged. In classical SOC estimation methods such as Amp-hour (Ah) balancing technique (**Hansen and Wang, 2005; Hicham et al., 2016; Caumont et al., 1998**) and Improved Ampere counting **(Dai et al., 2006; Shahriari and Farrokhi, 2013; Gholizadeh and Salmasi, 2014)**, the open circuit voltage (VOC) is considered due to the fact that battery voltage is directly correlated with the electrolytic concentration which varies with the battery charge status **(Chaoui et al., 2015)**. However, this approach suffers from accumulation of start-up and current sensor errors which results in a drift and bad accuracy **(Chaoui et al., 2015)**; while the latter can only be performed after a long rest of the battery when the battery is at equilibrium state **(Dai et al., 2006**), hence it is an undesirable strategy in practice.

Numerous studies have been performed on adaptive controllers for estimation of SOC **(Wang et al., 2015; Rahimi-Eichi et al., 2014; Shahriari and Farrokhi, 2014; Chaoui et al., 2015; Gholizadeh and Salmasi, 2014)**, the controllers were robust, but the input battery voltage was known beforehand. In **Chaoui et al. (2017)**, an adaptive estimation of battery parameters with post-temperature compensation was proposed over the Kalman filter; which is a recursive approach. Extended Kalman filter (EKF) was introduced in (**Chen et al., 2013; Watrin et al., 2012)** while considering the nonlinear behaviour of the VOC and the SOC. Direct use of sliding mode control (SMC) strategies for dc-dc converters have been extensively studied, such as given in (**Cardim et al., 2009; Vidal-Idiarte et al., 2009; Wai and Shih, 2011)**. Such a direct approach leads to an asymmetrical (variable) switching frequency of operation that is usually determined by the load **(Cardoso et al., 1992; Mattavelli et al., 1997)**. Therefore, in order to overcome the problems associated with asymmetrical switching, the sliding mode (SM) control techniques are transformed to equivalent modulating control input as applicable in a typical pulse width modulation (PWM) scheme with constant (symmetrical) switching frequency **(Tan et al., 2006; He and Luo, 2006; Mahdavi et al., 1997; Tan et al., 2007; Navarro-Lopez et al., 2009; Tan et al., 2008)**. In (**Sira-Ramirez et al., 1998; Fadil et al., 2006)**, The adaptive SMC was designed to deal with unknown load resistance. However, the input voltage must be pre-selected or pre-determined before the implementation of such control schemes.

In this paper, therefore, an adaptive SMC that is based on PWM with an observer scheme is used for the estimation of SOC and battery parameter nonlinearities to develop a robust charge control strategy on lithium ion batteries. In (**Oucheriah and Guo, 2013)**, the output of a dc-dc boost converter whose resistive load and external input are unknown is estimated only, with no consideration given to battery. Moreover, usually observers are not developed for both battery and connected dc-dc converter, as can be seen in (**Obeid et al., 2022; Barcellona et al., 2017**; **Wei et al., 2020);** where the parameter identifications were based on the battery alone. In the proposed controller the output voltage of the buck converter that charges the battery is unknown. Hence, a controller that estimates the converter output voltage and determines the control input is developed. The adaptive observer system developed is less sensitive to system parameter variation.

2. MATERIAL AND METHODS

The advantages of lithium-ion batteries over other batteries cannot be over emphasized, which include high power density and capacity for 80% dept of discharge. However, lithium-

ion batteries require complex electronic circuitries for controlling charge and discharge processes. In this Section, therefore, a model of lithium-ion battery is combined with a DC-DC buck converter; which is the power electronic circuit required for regulating the charging and discharging processes on the battery. Consequently, adaptive observers are introduced to estimate some of the battery's and the buck converter's parameters and variables for more robustness in the dynamic control. These parameters and variables are used to determine the SOC and SOH of the lithium-ion battery.

2.1 Model of Lithium-Ion Battery With Buck Converter

The lithium battery model in **(Hicham et al., 2016; Chen and Rincon-Mora; 2006)** is adopted in this study, which is connected to a DC-DC buck converter in **Fig. 1.** Consequently, an equivalent model of **Fig. 1** is given in **Fig. 2**.

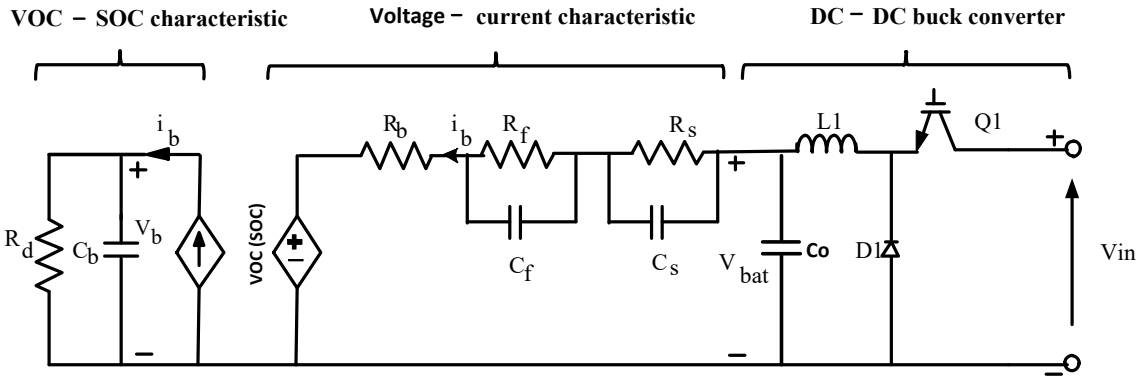

Figure 1. An electrical model connecting a lithium-ion battery to a dc-dc buck converter.

The model comprises of an internal battery's resistance R_b, and the RC network that represents fast and slow responses of the terminal voltage, which is modelled using resistances and capacitances R_s, C_s, R_f, *and* C_f. A voltage-controlled voltage source connects the internal resistance and RC network to the VOC-SOC characteristic of the battery, which is modelled by a current controlled current source, the battery storage capacity C_b, and the self-discharge resistance R_d.

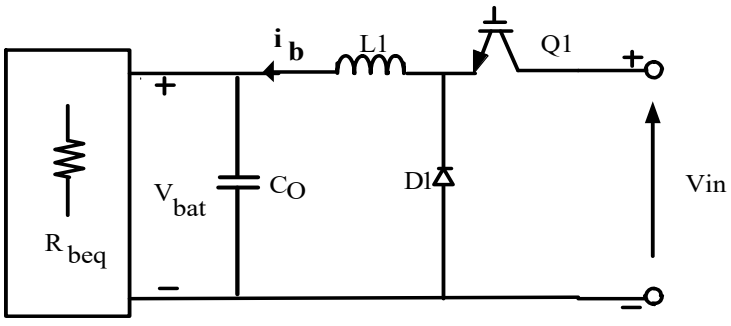

Figure 2. An equivalent block model of lithium-ion battery connected to a dc-dc buck converter

2.1.1 Dynamic Model for Observers

Let i_l, v_b, v_{bat}, θ represent the average inductor current, average whole capacitor voltage, average input battery voltage and inverse of battery equivalent resistance $\left(\theta = \frac{1}{R_{beq}}\right)$ respectively. Therefore, by applying Kirchhoff voltage and current laws to **Fig. 2**, Eqs. (1) and (2) are obtained as the averaged model of the battery-converter system.

$$pi_l = \frac{uV_{in}}{L} - \frac{v_{bat}}{L} \quad (1)$$

$$pv_{bat} = \frac{i_l}{C_o} - \frac{\theta v_{bat}}{C_o} \quad (2)$$

In Eqs. (1) and (2), $p = \frac{d}{dt}$, and the components L and C_o are the converter's inductor and output capacitor.

2.2 Estimation of Variables using Predetermined Battery Parameters for Adaptive Law

The estimator (observer) equations given in Eq. (3) and Eq. (4) are developed while considering the estimate for i_l, v_{bat}, θ as $\hat{\imath}_l, \hat{v}_{bat}, \hat{\theta}$ respectively.

$$p\hat{\imath}_l = \frac{u\hat{V}_{in}}{L} - \frac{\hat{v}_{bat}}{L} + K_1(i_l - \hat{\imath}_l) \quad (3)$$

$$p\hat{v}_{bat} = \frac{\hat{\imath}_l}{C_o} - \frac{\hat{\theta} v_{bat}}{C_o} + K_2(v_{bat} - \hat{v}_{bat}) \quad (4)$$

where the observer gains $K_1 > 0$ and $K_2 > 0$.

Let $\tilde{\imath}_l = i_l - \hat{\imath}_l$, $\tilde{v}_{bat} = v_{bat} - \hat{v}_{bat}$ and $\tilde{\theta} = \theta - \hat{\theta}$; therefore, Eq. (1) to Eq. (4) are used to obtain the following Eqs. (5) and (6).

$$p\tilde{\imath}_l = \frac{u\tilde{V}_{in}}{L} - \frac{\tilde{v}_{bat}}{L} - K_1\tilde{\imath}_l \quad (5)$$

$$p\tilde{v}_{bat} = \frac{\tilde{\imath}_l}{C_o} - \frac{\tilde{\theta} v_{bat}}{C_o} - K_2\tilde{v}_{bat} \quad (6)$$

Eq. (7) is developed as the Lyapunov function to obtain the adaptive laws, where $\gamma_1 > 0$ and $\gamma_2 > 0$ are design parameters. The stability criteria are that the derivative of Eq. (7) must be negative definite.

$$\tau = \frac{1}{2}L\tilde{\imath}_l^{\,2} + \frac{1}{2}C_o\,\tilde{v}_{bat}^{\,2} + \frac{1}{2\gamma_1}\tilde{\theta}^2 + \frac{1}{2\gamma_2}\tilde{V}_{in}^{\,2} \quad (7)$$

Then, the derivative of Eq. (7) with appropriate substitution from Eqs. (5) and (6) yields Eq. (8). Therefore Eq. (8) must be negative definite for stability to be guaranteed.

$$\dot{\tau} = -K_1L\tilde{\imath}_l^{\,2} - K_2C_o\tilde{v}_{bat}^{\,2} + \tilde{V}_{in}\left(u\tilde{\imath}_l - \frac{1}{\gamma_2}\dot{\hat{V}}_{in}\right) - \tilde{\theta}\left(v_{bat}\tilde{v}_{bat} + \frac{1}{\gamma_1}\dot{\hat{\theta}}\right) \quad (8)$$

The adaption law is determined by ensuring that the terms in brackets in Eq. (8) cancel out; therefore, such a condition will exist when Eq. (9) and Eq. (10) are fulfilled.

$$\dot{\hat{\theta}} = -\gamma_1 v_{bat}\tilde{v}_{bat} \quad (9)$$

$$\dot{\hat{V}}_{in} = u\gamma_2\tilde{\imath}_l \quad (10)$$

Therefore with Eq. (9) and Eq. (10) substituted in Eq. (8), Eq. (11) is obtained.

$$\dot{\tau} = -K_1 L\tilde{\imath}_l{}^2 - K_2 C_o\tilde{v}_{bat}{}^2 \quad (11)$$

2.3 Adaptive Sliding Mode Control using Predetermined Battery Parameters

In order to select a suitable sliding surface, the method given in (**Tan et al., 2006)** is adopted. However, in this case, Eq. (2) is set to zero to obtain the sliding surface of Eq. (12), whereby Eq. (2) is used to make appropriate substitution with $V_{bat} = V_{ref}$.

$$\sigma = \hat{\imath}_l - V_{ref}\hat{\theta} \quad (12)$$

By differentiating Eq. (12) with respect to time and equating it to zero and making appropriate substitution with Eqs. (5), (6) and (9), the equivalent control input is obtained in Eq. (13).

$$u_{eq} = \frac{\hat{v}_{bat} - LK_1\tilde{\imath}_l + \gamma_1 LV_{ref}v_{bat}\tilde{v}_{bat}}{\hat{V}_{in}} \quad (13)$$

2.4 Battery Parameter Estimation

The RC network of **Fig. 3** is an equivalent circuit network representation in **Fig. 2**; which is used for modelling the battery characteristics, where $R_f + R_s = R$.

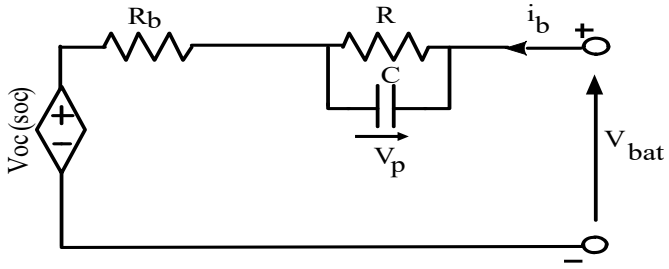

Fig. 3. The RC equivalent network.

The following assumptions as given in (**Hicham et al., 2016)** are used in deriving the dynamic equations:

Assumption 1: The battery's variables (voltage and current) along with their derivatives are continuous and bound.
Assumption 2: The observer's sampling frequency is set high enough such that $\dot{V}_{oc} \approx \dot{R} \approx \dot{C} \approx 0$.
The state equation for V_{bateq} (which is the terminal battery voltage V_{bat} using **Fig. 3**) is given in Eq. (14), while $\beta = \frac{1}{RC_{eq}}$.

$$pi_l = \beta V_{bateq} + R_b i_l - \beta(R + R_b) i_l - \beta V_{oc} \quad (14)$$

2.5 Estimation of Buck Converter Variables and Battery Parameters for Adaptive Laws

An estimator equation for Eq. (14) is developed in Eq. (15) with the variables $\hat{\imath}_l, \hat{v}_b, and\ \hat{v}_{bat}$ representing estimates. The state error derived from Eqs. (14) and (15) is given in Eq. (16).

$$p\hat{v}_{bateq} = \hat{\beta} v_{bateq} + \hat{R}_b p\hat{\imath}_l - \hat{\beta}(\hat{R} + \hat{R}_b)\hat{\imath}_l - \hat{\beta}\hat{V}_{oc} + K_3(v_{bat} - \hat{v}_{bat}) \quad (15)$$

$$p\tilde{v}_{bateq} = \tilde{\beta} v_{bateq} + \tilde{R}_b p\tilde{\imath}_l - \tilde{\beta}(\tilde{R} + \tilde{R}_b)\tilde{\imath}_l - \tilde{\beta}\tilde{V}_{oc} - K_3\tilde{v}_{bat} \quad (16)$$

Therefore, Lyapunov function candidate of Eq. (17) is derived.

$$\tau = \frac{L}{2}\tilde{\imath}_l^{\,2} + \frac{C_b}{2}\tilde{v}_{bat}^{\,2} + \frac{1}{2\gamma_3}\tilde{v}_{bateq}^{\,2} + \frac{1}{2\gamma_4}\tilde{V}_{oc}^{\,2} + \frac{1}{2\gamma_5}\tilde{R}_b^{\,2} + \frac{1}{2\gamma_6}\tilde{R}^2 + \frac{1}{2\gamma_7}\tilde{\theta}^2 + \frac{1}{2\gamma_8}\tilde{V}_{in}^{\,2} + \frac{1}{2\gamma_9}\tilde{\beta}^2 \quad (17)$$

where $\gamma_3, \gamma_4, \gamma_5, \gamma_6, \gamma_7, \gamma_8, \gamma_9 > 0$are design parameters.
The derivative of Eq. (17) while making appropriate substitution and simplification with Eq. (16) yields Eq. (18).

$$\dot{\tau} = L\tilde{\imath}_l\left[\frac{u\tilde{V}_{in}}{L} - \frac{\tilde{v}_{bat}}{L} - K_1\tilde{\imath}_l\right] + C_o\tilde{v}_{bat}\left[\frac{\tilde{\imath}_l}{C_o} - \frac{\tilde{\theta}v_{bat}}{C_o} - K_2\tilde{v}_{bat}\right] - \frac{1}{\gamma_4}\tilde{V}_{oc}\dot{\tilde{V}}_{oc} - \frac{1}{\gamma_5}\tilde{R}_b\dot{\tilde{R}}_b + \frac{1}{\gamma_3}\tilde{v}_{bateq}\left[\tilde{\beta}v_{bateq} + \tilde{R}_b\left[\frac{u\tilde{V}_{in}}{L} - \frac{\tilde{v}_b}{L} - K_1\tilde{\imath}_l\right] - \tilde{\beta}(\tilde{R} + \tilde{R}_b)\tilde{\imath}_l - \tilde{\beta}\tilde{V}_{oc} - K_3\tilde{\imath}_l\right] - \frac{1}{\gamma_6}\tilde{R}\dot{\tilde{R}} - \frac{1}{\gamma_7}\tilde{\theta}\dot{\tilde{\theta}} - \frac{1}{\gamma_8}\tilde{V}_{in}\dot{\tilde{V}}_{in} - \frac{1}{\gamma_9}\tilde{\beta}\dot{\tilde{\beta}} \quad (18)$$

Eq. (18) is ensured to be negative definite to fulfill Lyapunov stability criteria. Hence, the adaptive laws given in Eqs. (19) to (24) are obtained.

$$\dot{\tilde{\theta}} = -\gamma_7 v_{bat}\tilde{v}_{bat} \quad (19)$$

$$\dot{\tilde{R}}_b = \frac{\gamma_5}{\gamma_3}\tilde{v}_{bateq}\left[\frac{u\tilde{V}_{in}}{L} - \frac{\tilde{v}_{bat}}{L} - K_1\tilde{\imath}_l\right] - \gamma_5\tilde{\beta}\tilde{\imath}_l \quad (20)$$

$$\dot{\tilde{V}}_{in} = \gamma_8 u\left[\tilde{\imath}_l + \frac{\tilde{v}_{bateq}}{\gamma_3}\tilde{R}_b\frac{1}{L}\right] \quad (21)$$

$$\dot{\tilde{R}} = -\frac{\gamma_6}{\gamma_3}\tilde{\beta}\tilde{\imath}_l\tilde{v}_{bateq} \quad (22)$$

$$\dot{\tilde{V}}_{oc} = -\gamma_4\tilde{v}_{bateq}\tilde{\beta} \quad (23)$$

$$\dot{\tilde{\beta}} = \gamma_9\tilde{v}_{bateq}\left[\frac{1}{\gamma_3}v_{bat} - (\tilde{R} + \tilde{R}_b)\tilde{\imath}_l - \tilde{V}_{oc}\right] \quad (24)$$

Therefore, with Eqs. (19) through (24) substituted back into Eq. (18), Eq. (25) is obtained.

$$\dot{\tau} = -K_1 L\tilde{\imath}_l^{\,2} - K_2 C_o\tilde{v}_{bat}^{\,2} \quad (25)$$

2.6 Adaptive Sliding Mode Control Scheme using Estimated Battery Parameters

Similarly, the sliding surface in Eq. (26) is obtained by equating Eq. (14) to zero; Eq. (27) is obtained as the equivalent control input. Eq. (27) is normalized to $0 < u_{eq} < 1$. Therefore, pulse width modulation (PWM) is realized by utilizing the u_{eq} to modulate a single sided triangular carrier signal to generate the switching pulses for the DC-DC buck converter. The advantage of the PWM based sliding mode control is that the switching of the DC-DC converter becomes symmetrical with a defined switching frequency by the carrier signal. Conventional sliding mode control utilizing hysteresis controller gives asymmetrical switching frequency, which may yield harmonics at the output of the DC-DC converter that will not be healthy for charging the lithium-ion battery.

$$\sigma = i_l - \frac{V_{ref} - \hat{V}_{oc}}{(\hat{R} + \hat{R}_b)} \tag{26}$$

$$u_{eq} = \frac{\hat{v}_{bat} - LK_1\tilde{\imath}_l - LV_{ref}E_1 - LE_2}{\hat{V}_{in}} = \frac{\hat{v}_{bat} - LK_1\tilde{\imath}_l + \gamma_1 LV_{ref}v_{bat}\tilde{v}_{bat}}{\hat{V}_{in}} \tag{27}$$

$$E_1 = \frac{\dot{\hat{R}} + \dot{\hat{R}}_b}{(\hat{R} + \hat{R}_b)^2} \tag{28}$$

$$E_2 = \frac{\dot{\hat{V}}_{oc}(\hat{R} + \hat{R}_b) - \hat{V}_{oc}\left(\dot{\hat{R}} + \dot{\hat{R}}_b\right)}{(\hat{R} + \hat{R}_b)^2} \tag{29}$$

Assumption 3: Since Eq. (10) is equal to Eq. (21), Eq. (30) is obtained.

$$\tilde{R}_b = (\gamma_2 - \gamma_8)\frac{L\tilde{\imath}_l\gamma_1}{\tilde{v}_{bat}} \tag{30}$$

Also, equating Eqs. (13) to (27) which suggest equal control input yields Eqs. (31) and (32), while substituting Eq. (23) in Eq. (32) yields Eq. (33).

$$V_{ref} = \hat{V}_{oc} \tag{31}$$

$$\gamma_1 V_{ref}\left(\hat{R} + \hat{R}_b\right)v_{bat}\tilde{v}_{bat} = -\dot{\hat{V}}_{oc} \tag{32}$$

$$\tilde{\beta} = \frac{\gamma_1 V_{ref}(\hat{R} + \hat{R}_b)v_{bat}}{\gamma_4} \tag{33}$$

Equating Eq. (6) and Eq. (16) gives Eq. (34).

$$\tilde{R} = \frac{1}{\tilde{\beta}C_b} - \tilde{R}_b \tag{34}$$

2.7 Selection of Gains

The PWM adaptive sliding controller with estimated battery parameters will be asymptotically stable when $\tilde{\imath}_l \to 0, \tilde{v}_{bat} \to 0$. Therefore, substituting Eqs. (3), (4), (12), and (27) into Eq. (15) yields Eq. (35), which is rearranged as Eq. (36).

$$p\hat{v}_{bateq} = \hat{\beta}\hat{v}_{bateq} - \hat{R}_b\frac{\hat{v}_{bat}}{L} + \hat{R}_b K_1\tilde{\imath}_l - \hat{\beta}\hat{v}_{oc} + K_3\tilde{v}_{bat} + \hat{R}_b\frac{\hat{V}_{in}}{L}\left(\frac{\hat{v}_{bat} - LK_1\tilde{\imath}_l - LV_{ref}E_1 - LE_2}{\hat{V}_{in}}\right) - \hat{\beta}(\hat{R}+\hat{R}_b)\hat{\theta}\hat{V}_{in}\left(\frac{\hat{v}_{bat} - LK_1\tilde{\imath}_l - LV_{ref}E_1 - LE_2}{\hat{V}_{in}}\right) \quad (35)$$

$$p\hat{v}_{bateq} = \hat{\beta}\hat{v}_{bateq} + \hat{R}_b\frac{\hat{v}_{bat}}{L} - \hat{R}_b\frac{\hat{v}_{bat}}{L} - \hat{\beta}(\hat{R} + \hat{R}_b)\hat{\theta}\hat{v}_{bat} - \hat{\beta}\hat{V}_{oc} + \varphi \quad (36)$$

Since $\hat{V}_{oc} \to V_{ref}$, therefore Eq. (37) evolves from Eq. (36).

$$p\hat{v}_{bat} = \hat{\beta}\left[(1 - (\hat{R}+\hat{R}_b)\hat{\theta})\hat{v}_{bat} - \hat{V}_{oc}\right] + \varphi \quad (37)$$

Solving Eq. (37) to validate assumption 3 yields

$$\hat{R} = -\hat{R}_b \quad (38)$$

$$p\hat{v}_{bat} = \hat{\beta}\left[\hat{v}_{bat} - \hat{V}_{oc}\right] + \varphi \quad (39)$$

where $\hat{\beta}$ is a gain multiplier for the selection of K_3. K_1 and K_2 can be selected as given in (**Oucheriah and Guo, 2013**).

$$\varphi = \hat{\beta}\tilde{v}_{bat} + \hat{R}_b(K_1\tilde{\imath}_l - K_1\tilde{\imath}_l - v_{ref}E_1 - LE_2) + \hat{\beta}(\hat{R}+\hat{R}_b)L\hat{\theta}(K_1\tilde{\imath}_l + V_{ref}E_1 + E_2) + K_3\tilde{v}_{bat} \quad (40)$$

Since $\varphi \to 0\ as\ \tilde{\imath}_l \to 0, \tilde{v}_{bat} \to 0$, the solution to Eq. (35) is asymptotically stable and converges towards $\hat{v}_{bat} = V_{ref}$ when $\hat{R} = -\hat{R}_b$ with an approximate exponential rate $\hat{\beta}$. **Fig. 4** illustrates the overall strategy for the controller.

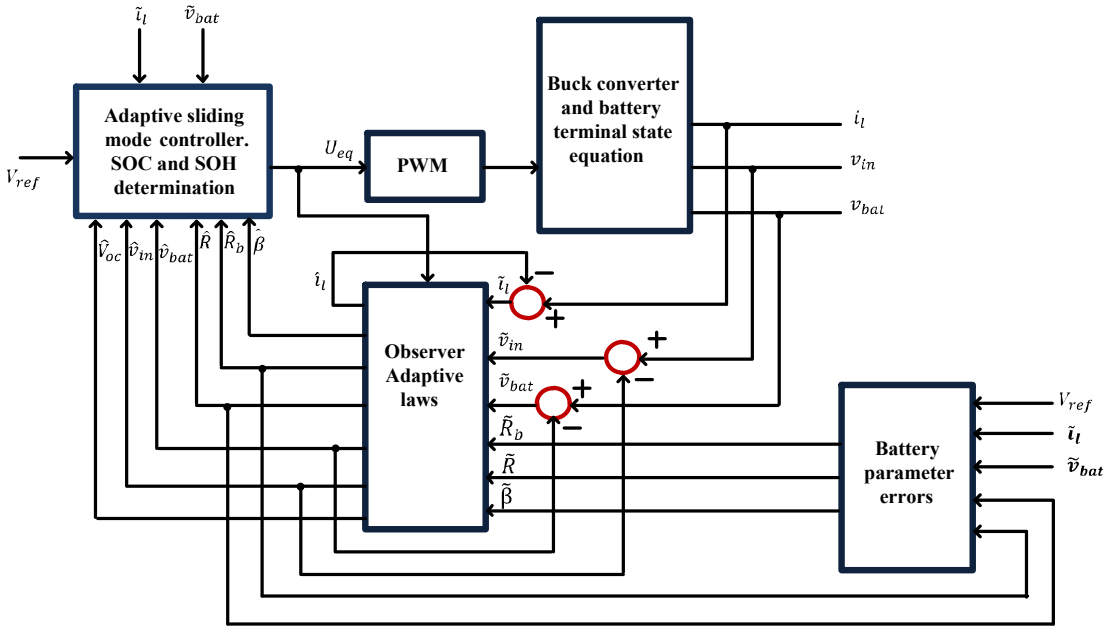

Figure 4. Block diagram for the implementation of the proposed controller.

3. SIMULATION RESULTS AND DISCUSSION

The adaptive observers and dynamic control schemes presented were simulated in MATLAB/SIMULINK environment. Results obtained from the simulation are presented in this Section.

The initial conditions of the observer are chosen as $\hat{\imath}_l(0) = 0.8, \hat{v}_b(0) = 2.6, \hat{\mathrm{v}}_{\mathrm{bat}}(0) = 2.6, \hat{\mathrm{V}}_{\mathrm{oc}}(0) = 2.2$, and the adaptive laws $\hat{R}_b(0)$, $\hat{R}(0)$, $\hat{\beta}(0)$, $\hat{\theta}(0)$ can be selected to initiate the occurrence of sliding mode, which must be chosen such that the sliding mode starts at $t = 0$, i.e.

$$(0) = \hat{\imath}_l(0) - V_{ref}\hat{\theta}(0) = 0, \quad \hat{\theta}(0) = 0.1905$$

$$\sigma(0) = \hat{\imath}_l(0) - \left(\left(V_{ref} - \hat{v}_{oc}(0)\right)/\left(\hat{R}(0) + \hat{R}_b(0)\right)\right) = 0, \qquad \hat{R} + \hat{R}_b = 2.5.$$

The open circuit voltage is linearly related to the SOC, as given in (**Rahimi-Eichi et al., 2013)**, by Eq. (41).

$$V_{oc} = b_0 + b_1 SOC = \left(\frac{b_0}{SOC} + b_1\right) SOC = b'SOC \tag{41}$$

If SOC is normalization from 0 to 1, we can use the following general normalization stated in Eq. (42) to predict SOC.

$$\hat{V}_{oc}(t) = b' \frac{\hat{\mathrm{v}}_{\mathrm{bat}}}{V_{batmax}} = b(t)\hat{\mathrm{v}}_{\mathrm{bat}} \tag{42}$$

When Eq. (42) is substituted in Eq. (16) and compared with Eq. (3), Eqs. (43) and (44) are obtained

$$\hat{\beta}(t) = \frac{C_o(1-b(t))}{\hat{\theta}(t)} \tag{43}$$

$$\left(\hat{R}(t) + \hat{R}_b(t)\right) = \frac{\hat{\beta}(t)}{C_o} \tag{44}$$

With the appropriate substitution with Eqs. (43) and (44), Eq. (40) is obtained.

$$b(t) = 1 - \left(\hat{R}(t) + \hat{R}_b(t)\right)\hat{\theta}(t) \tag{45}$$

Note that $b(t)$ is a normalization that relates $\hat{\mathrm{v}}_{\mathrm{bat}}$ to $\hat{V}_{oc}$(t), so the rescaling of $b(t)$ is SOC; therefore $b(0) = 0.6191, \hat{\beta}(0) = 4.799 \times 10^{-5}$.

The overall control strategy is simulated in the Simulink in the MATLAB environment. The outcomes obtained from the simulation are represented graphically in **Figs. 5** to **12**. The presented results are given to span from simulation start-up time 0 s till 1000s to reveal both the constant current charging mode and the constant voltage charging mode. Usually, there are three modes in charging lithium ion batteries, namely constant current, cell equalization, and constant voltage modes. Since a single cell is used in this study the cell equalization mode is not required.

In **Fig. 5**, the robustness of the observer model for the converter's input voltage is demonstrated. Since the converter is a buck converter, its input is greater than its output that is used to charge the lithium-ion battery. Consequently, it is shown in **Fig. 5** that the observed (estimated) converter's input voltage tracked the set reference voltage with an insignificant error margin.

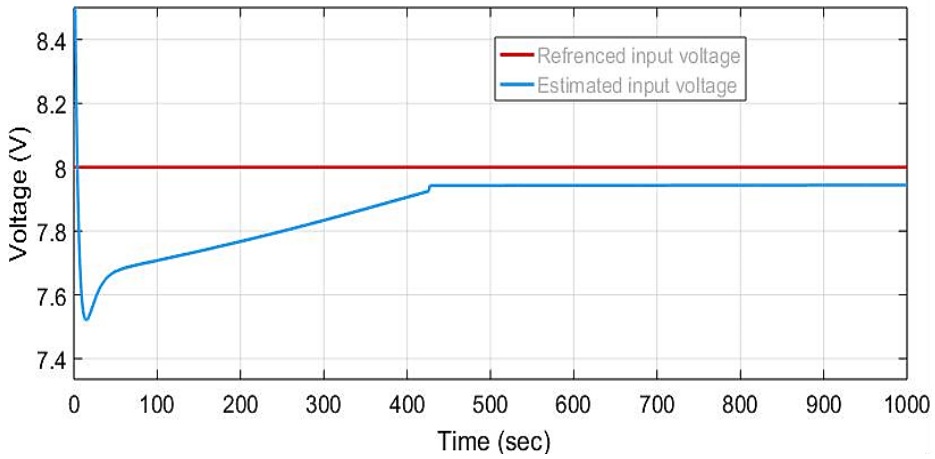

Figure 5. Reference and estimated input converter voltage

Fig. 6 gives the self-discharging resistance; which is considered as the Load. In the figure, it is evident that the sliding mode controller has robust recovery features to sudden variations in input and un-modelled load. Therefore, when the algorithm converges correctly it can be used to know the exact value of the self-discharging resistance. **Fig. 7** shows the current which tracks the reference current even with initial guess and sudden input variations.

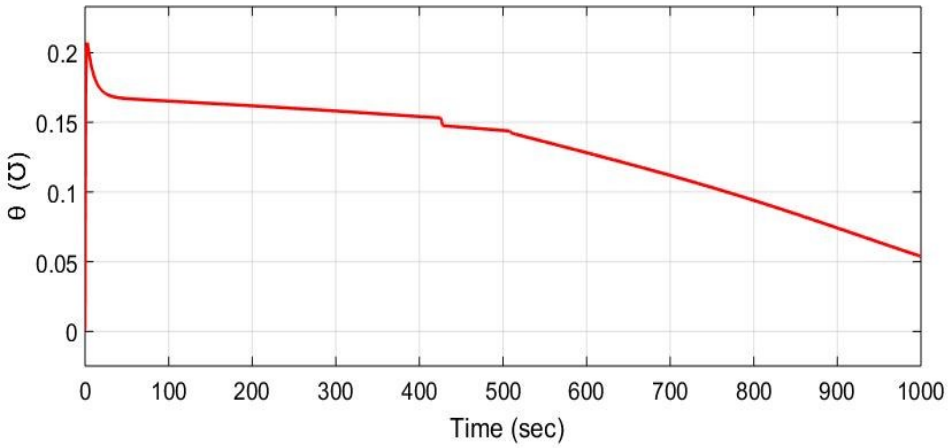

Figure 6. Estimated inverse of total battery equivalent resistance.

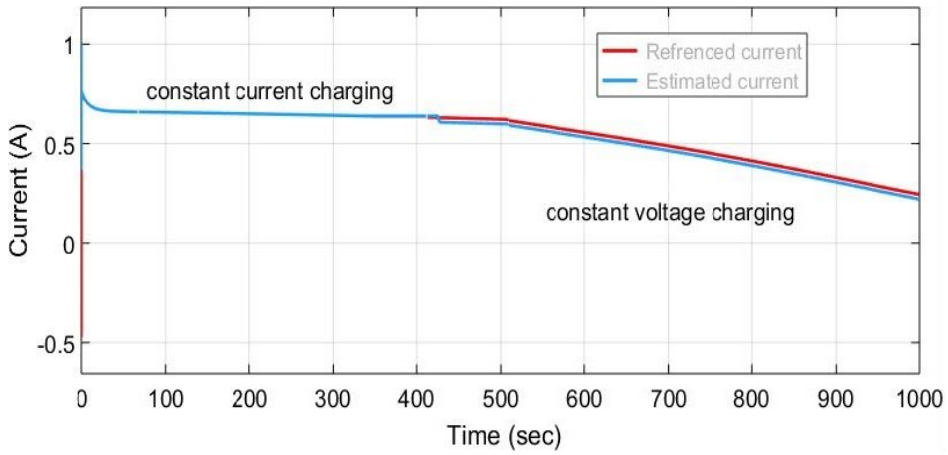

Figure 7. Reference and estimated Currents

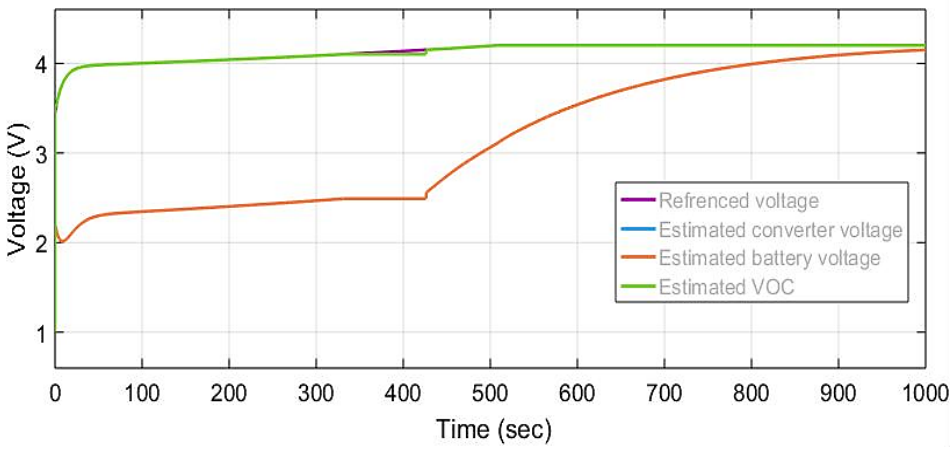

Figure 8. Terminal voltage and open circuit voltage V_{oc}

Fig. 8 shows the estimated converter's output terminal voltage and estimated open circuit voltage (VOC), which follow the reference voltage closely. In order for the battery to be fully charged the value of the battery terminal voltage must be equal or approximately equal to the open circuit voltage after charge i.e. the battery is at equilibrium. Therefore, in **Fig. 8** it is seen that the estimated battery voltage charges to the reference converter's output voltage to reach 100% SOC. **Fig. 9** gives the β Plot, which gives the exact value for the gain and this value can be utilized to determine the equivalent capacitance of the RC network which is used for modelling of the battery.

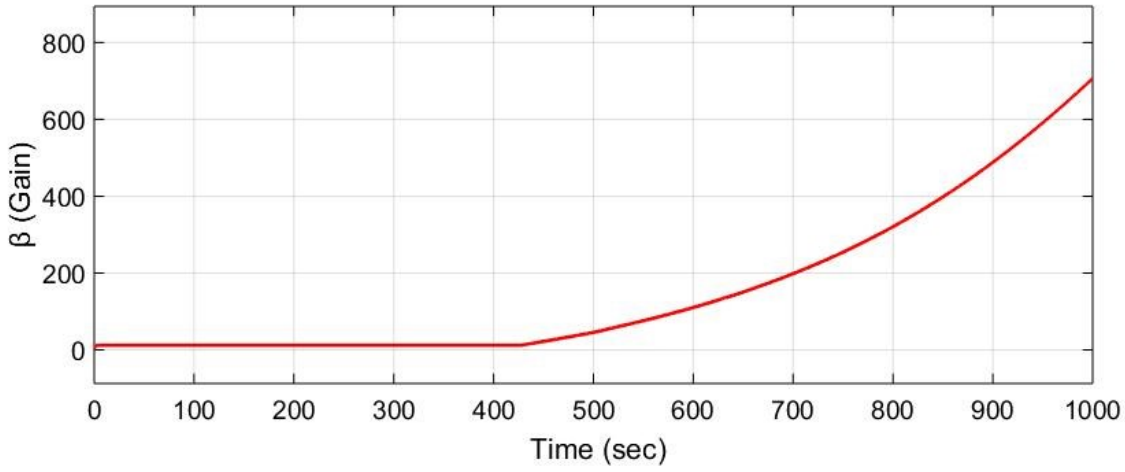

Figure 9. β Plot with ti.

In (**Hicham et al., 2016)**, it was reported that increase in the battery's equivalent series resistance R_{bat} is an indication of SOH decline (where $R_{bat} = R_b + R_f + R_s = R_b + R$). Consequently, **Fig. 10** validates Eq. (34) such that when the summation of R_b and R is small then a good SOH is established, and the battery can recover its 100% SOC.

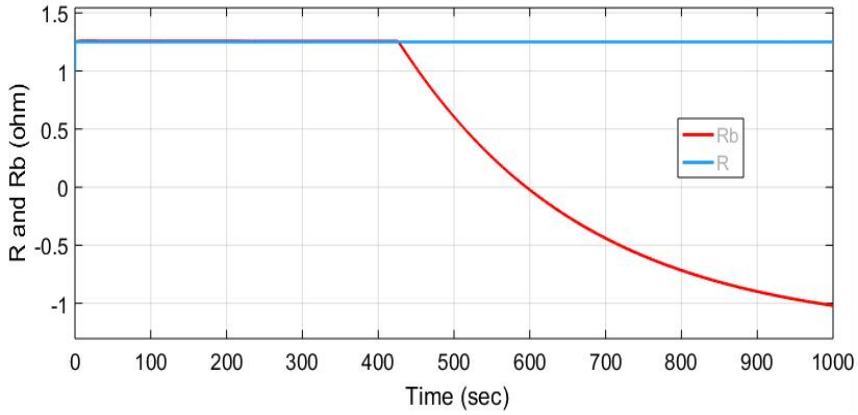

Figure 10. Series and equivalent battery resistance

Fig. 11 gives the SOC, and shows the variation of the SOC to the open circuit voltage VOC. As the SOC of the battery increases, the VOC also increases until 100% SOC is reached. The figure also shows that for the battery to be fully charged to maximum then the VOC would have reached 4.19999V.

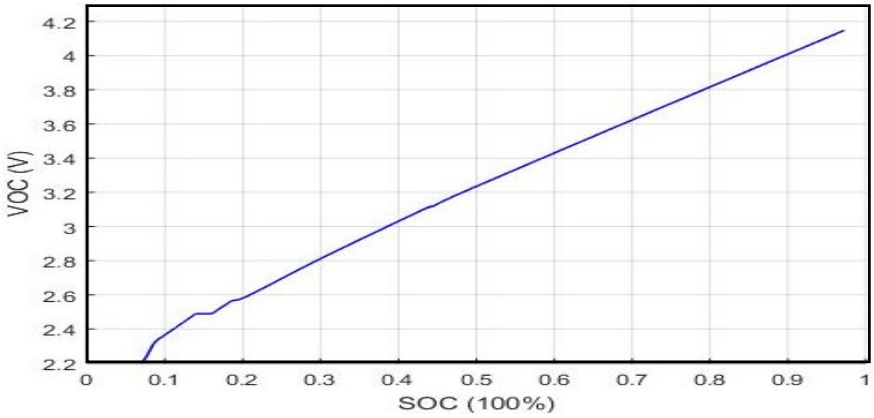

Figure 11. State of charge

Finally, for the proposed schemes, with or without battery parameters to be effective, the sliding surfaces must be zero or tend to zero as implied by Eqs. (12) and (24), which is shown in **Fig. 12**.

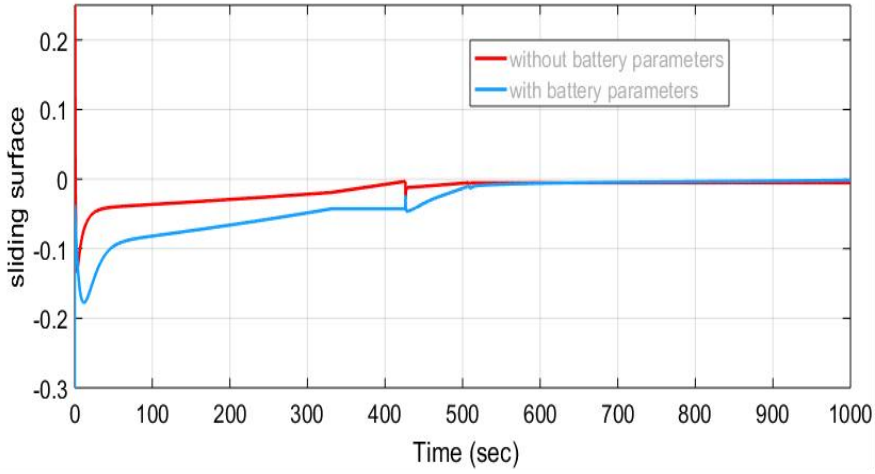

Figure 12. Sliding surface

4. CONCLUSION

A PWM-observer based adaptive sliding mode control scheme has been designed for a dc-dc buck converter to estimate the input battery voltage and the battery parameters for the purpose of achieving robust charge control on lithium ion batteries. Simulation was done to transition from constant current charging mode to constant voltage charging mode. The results obtained from both modes have shown that the dynamic control system of the SMC is asymptotically stable with excellent robust recovery features to sudden variations in input and un-modelled load. Therefore, the methods proposed in this paper achieved its set objectives.

5. NOMENCLATURE

Symbol	Description	Symbol	Description
C_b	Battery storage capacity	i_l	Average inductor current
C_f	Fast response resistance in battery model	v_b	Average whole capacitor voltage
C_s	Slow response capacitance in battery model	v_{in}	Voltage input to the DC-DC buck converter
R_b	Battery's internal resistance	v_{bat}	Average input battery voltage
R_d	Self-discharge resistance	SOC	State of charge
R_f	Fast response resistance in battery model	SOH	State of health
R_s	Slow response resistance in battery model	VOC	Open circuit voltage
		θ	Inverse of battery equivalent resistance

Acknowledgments

The authors are thankful for the resources rendered by the Department of Electrical and Electronics Engineering, Faculty of Engineering, University of Lagos, Lagos, Nigeria; which substantially helped this study.

Credit Authorship Contribution Statement

Adeola Balogun: Writing–original draft, review & editing, Validation. Chukwuemeka Sunday: Methodology, Data collection, Sunday Adetona: Writing–review & editing, Validation. Agoro Sodiq: Writing –review & editing, Frank Okafor: Writing-review & editing.

Declaration of Competing Interest

The authors declare that they have no known competing financial interests or personal relationships that could have appeared to influence the work reported in this paper

REFERENCES

Barcellona, S. and Piegari, L., 2017, Lithium ion battery models and parameter identification techniques. *Energies*, 10(12), p.2007. https://doi.org/10.3390/en10122007

Cardim R., Teixeira M. C. M., Assuno E., and Covacic M. R., 2009, Variable-structure control design of switched systems with an application to a dc–dc power converter, *IEEE Trans. Ind. Electron.*, 56(9), pp. 3505–3513. https://doi.org/10.1109/TIE.2009.2026381

Cardoso B. J., Moreira A. F., Menezes B. R., and Cortizo P. C., 1992, Analysis of switching frequency reduction methods applied to sliding mode controlled dc–dc converters, *Proc. IEEE Appl. Power Electron. Conf. Expo*, pp. 403–410. https://doi.org/10.1109/APEC.1992.228382

Caumont, O., Le Moigne, P. P., and Lenain, C., 1998, An Optimized state of charge algorithm for lead acid batteries in electric vehicles, *Proc. Electric Vehicle Symposium*, Brussels, Belgium, Vol. EVS-15.

Chaoui H., Elmejdoubi A., and Gualous H., 2017, Online parameter identification of lithium-ion batteries with surface temperature cells, *IEEE Transactions on Vehicular Technology*, 66(3), pp. 2000–2009. https://doi.org/10.1109/TVT.2016.2583478

Chaoui H., Golbon N., Hmouz I., Souissi R., and Tahar S., 2015, Lyapunov-based adaptive state of charge and state of health estimation for lithium-ion batteries, *IEEE Transactions on Industrial Electronics,* 62(3), pp. 1610–1618. https://doi.org/10.1109/TIE.2014.2341576

Chen M., and Rincon-Mora G. A., 2006, Accurate electrical battery model capable of predicting run-time and I-V performance, *IEEE Transaction on Energy Conversion*, 21(2), pp. 504-511. https://doi.org/10.1109/TEC.2006.874229

Chen Z., Fu Y., and Mi C., 2013, State of charge estimation of lithium-ion batteries in electric drive vehicles using extended Kalman filtering, *IEEE Transactions on Vehicular Technology,* 62(3), pp. 1020–1030. https://doi.org/10.1109/TVT.2012.2235474

Dai, H., Sun Z., and Wei, X., 2006, Online SOC estimation of high-power lithium-ion batteries used on HEV's, *Proc. IEEE Int. Conf. Vehicle Electron. Safety,* pp. 342-347. https://doi.org/10.1109/ICVES.2006.371612

El Fadil H., Giri F., and Ouadi H., 2006, Adaptive sliding mode control of PWM boost dc–dc converters, *Proc. IEEE Int. Conf. Control Appl.,* Munich, Germany, pp. 3151–3156. https://doi.org/10.1109/CACSD-CCA-ISIC.2006.4777142

Gholizadeh M., and Salmasi F., 2014, Estimation of state of charge, unknown nonlinearities, and state of health of a lithium-ion battery based on a comprehensive unobservable model, *IEEE Transactions on Industrial Electronics,* 61(3), pp. 1335–1344. https://doi.org/10.1109/TIE.2013.2259779

Hansen T., and Wang, C.J., 2005, Support vector based battery state of charge estimator, *Journal of Power Sources,* 141(2), pp. 351–358. https://doi.org/10.1016/j.jpowsour.2004.09.020

He Y., and Luo F. L., 2006, Sliding-mode control for dc–dc converters with constant switching frequency, *Inst. Elect. Eng. Proc. Control Theory Appl.,* 153(1), pp. 37–45. https://doi.org/10.1049/ip-cta:20050030

Kim, I., 2010, A Technique for estimating the state of health of lithium batteries through a dual-sliding-mode observer, *IEEE Transactions on Power Electronics,* 25, (4), pp. 1013 - 1022. https://doi.org/10.1109/TPEL.2009.2034966

Mahdavi, J., Emadi A., and Toliyat H. A., 1997, Application of state-space averaging method to sliding mode control of PWM dc/dc converters, *Proc. IEEE Ind. Appl. Soc. Annu. Meeting*, 2, pp. 820–827. https://doi.org/10.1109/IAS.1997.628957

Mattavelli P., Rossetto L., and Spiazzi G., 1997, Small-signal analysis of dc–dc converters with sliding mode control, *IEEE Trans. Power Electron*, 12(1), pp. 96–102. https://doi.org /10.1109/63.554174

Navarro-Lopez E. M., Cortes D., and Castro C., 2009, Design of practical sliding-mode controllers with constant switching frequency for power converters, *Elect. Powers Syst. Res.,* 79(5). pp. 796–802. https://doi.org/10.1016/j.epsr.2008.10.018

Obeid, H., Petrone, R., Chaoui, H., and Gualous, H. 2022, Higher order sliding-mode observers for state-of-charge and state-of-health estimation of lithium-ion batteries, *IEEE Transactions on Vehicular Technology*, 72(4), pp. 4482-4492. https://doi.org/10.1109/TVT.2022.3226686

Oucheriah S., and L. Guo L., 2013, PWM- based adaptive sliding-mode control for dc-dc boost power converter, *IEEE Transactions on Industrial Electronics*, 60(8), pp. 3291-3294. https://doi.org/10.1109/TIE.2012.2203769

Rahimi-Eichi H., Baronti F., and Chow M.Y., 2014, Online adaptive parameter identification and state-of-charge coestimation for lithium-polymer battery cells, *IEEE Transactions on Industrial Electronics,* 61(4), pp. 2053–2061. https://doi.org/10.1109/TIE.2013.2263774

Shahriari, M., and Farrokhi, M., 2013, Online state-of-health estimation of VRLA batteries using state of charge, *IEEE Transactions on Indus- trial Electronics,* 60(1), pp. 191–202. https://doi.org/10.1109/TIE.2012.2186771

Sira-Ramirez H., Ortega R, and Garcia-Esteban M, 1998, Adaptive passivity based control of average dc-to-dc power converter models, *Int. J. Adapt. Control Signal Process*, 12(1), pp. 63–80.

Tan S. T., Lai Y. M., and Tse C. K., 2006 A unified approach to the design of PWM-based sliding-mode controllers for basic dc–dc converters in continuous conduction mode, *IEEE Trans. Circuits Syst.,* 53(8), pp. 1816–1827. https://doi.org/10.1109/TCSI.2006.879052

Tan S. T., Lai Y. M., and Tse C. K., 2008, General design issues of sliding-mode controllers in dc–dc converters, *IEEE Trans. Ind. Electron.,* 55(3), pp. 1160–1174. https://doi.org/10.1109/TIE.2007.909058

Tan S. T., Lai Y. M., Tse C. K., Martinez-Salamero L., and Wu C. K., 2007, A fast-response sliding-mode controller for boost-type converters with a wide range of operating conditions, *IEEE Trans. Ind. Electron.*, 54(6), pp. 3276–3286. https://doi.org/10.1109/TIE.2007.905969

Vidal-Idiarte E., Carrejo C. E., Calvente J., and Martinez-Salamero L., 2011, Two-loop digital sliding mode control of dc–dc power converters based on predictive interpolation, *IEEE Trans. Ind. Electron.,* 58(6), pp. 2491–2501. https://doi.org/10.1109/TIE.2010.2069071

Wai R.J., and Shih L.C., 2011, Design of voltage tracking control for dc–dc boost converter via total sliding-mode technique, *IEEE Trans. Ind. Electron*., 58(6), pp. 2502–2511. https://doi.org/10.1109/TIE.2010.2066539

Wang Y., Fang H., Sahinoglu Z., Wada T., and Hara S., 2015, adaptive estimation of the state of charge for lithium-ion batteries: nonlinear geometric observer approach, *IEEE Transactions on Control Systems Technology,* 23(3), pp. 948–962. https://doi.org/10.1109/TCST.2014.2356503

Watrin N., Roche R., Ostermann H., Blunier B., and Miraoui A., 2012, Multiphysical lithium-based battery model for use in state-of-charge determination, *IEEE Transactions on Vehicular Technology*, 61(8), pp. 3420–3429. https://doi.org/10.1109/TVT.2012.2205169

Wei, Z., Zhao, D., He, H., Cao, W. and Dong, G., 2020, A noise-tolerant model parameterization method for lithium-ion battery management system, *Applied Energy*, 268, p.114932. https://doi.org/10.1016/j.apenergy.2020.114932

مراقب وضع الانزلاق التكيفي PWM للتحكم في شحن بطارية ليثيوم أيون

أديولا بالوغون[1]، تشوكويميكا الأحد[1]، الأحد أديتونا[1]*، صديق أغورو[2] ، فرانك أوكافور[3]

[1]قسم الهندسة الكهربائية والإلكترونية، جامعة لاغوس، لاغوس، نيجيريا

[2]شركة ايه بي بي .رالي نورث كارولاينا الولايات المتحدة الأمريكية، نورث كارولاينا، الولايات المتحدة الأمريكية

[3]هيئة تنظيم الكهرباء النيجيرية، أبوجا، نيجيريا

خلاصة

يُقترح التحكم في وضع الانزلاق التكيفي (SMC) استنادًا إلى PWM ونظام مراقب للتنبؤ بحالة الشحن (SOC) لبطارية أيون الليثيوم . تم تطوير نظام التحكم لمحول باك DC-DC المستخدم في التحكم المنظم في شحن بطاريات الليثيوم أيون .على عكس العديد من مخططات التقدير حيث يتم تحديد جهد خرج المحول مسبقًا وتجاهل اللاخطيات، فإن المخطط المقترح يقدر جهد خرج محول باك، وSOC، واللاخطية من حيث الأخطاء في المعلمات .يتم ضمان استقرار المخطط المقترح بطريقة ليابونوف .تم إجراء المحاكاة في Simulinkفي بيئة MATLAB من أجل الانتقال من وضع الشحن الحالي الثابت إلى وضع الشحن ذو الجهد الثابت .أظهرت النتائج التي تم الحصول عليها من كلا الوضعين في Simulink في بيئة MATLAB أن نظام التحكم الديناميكي لـ SMC مستقر بشكل مقارب مع ميزات استرداد قوية ممتازة للتغيرات المفاجئة في الإدخال والحمل غير النموذجي.

الكلمات المفتاحية :التحكم التكيفي في الوضع المنزلق، محولdc-dc ، بطارية ليثيوم أيون، ثباتLyapunov ، حالة الشحن